# X-ray microtomography as a visualization tool for fluid-rock interaction in the oceanic crust: insights into serpentinisation and low-temperature seawater alteration

W.-A. Kahl, N. Jöns

Geosciences Department, University of Bremen, Klagenfurter Straße, 28359 Bremen, Germany, wakahl@uni-bremen.de

## Aims

Serpentinites are products of hydrous alteration of ultramafic mantle rocks (i.e. peridotites). Particularly at slow-spreading mid-oceanic ridges, tectonic faulting leads to exposure of these mantle-derived peridotites at the seafloor, where they are exposed to interaction with seawater. Already during uplift from greater depth, seawater-derived fluids present on shear zones lead to serpentinisation when temperatures drop below □350-400 °C. While the original peridotite consists mainly of anhydrous minerals such as olivine and orthopyroxene (depending on the proportion of these two minerals, the rocks are named either dunite or harzburgite), the serpentinite that results from seawater-peridotite interaction shows a completely different mineralogy. Serpentinites consist predominantly of serpentine group minerals (hydrous Mg-Fe silicates) + magnetite (a ferrimagnetic spinel) ± brucite (a Mg-Fe hydroxide). In recent years the process of serpentinisation sparked interest, because it has significant consequences for the physical properties and chemical composition of the oceanic lithosphere. Furthermore, serpentinisation reactions lead to release of dihydrogen ($H_2$), which is an energy source for chemosynthetic life in the deep sea. Hydrogen is produced when $H_2O$ oxidises ferrous iron ($Fe^{2+}$) in primary minerals (i.e. olivine and orthopyroxene) to ferric iron ($Fe^{3+}$) in secondary phases (mainly magnetite). Detailed determination of the volumetric proportions of secondary minerals is crucial for estimating chemical budgets related to serpentinisation processes. Moreover, in these systems, fluid infiltration, fluid-rock interaction and reaction progress are strongly coupled with the hydrodynamic behaviour. Changes of permeability due to large reaction volumes and heterogeneous pore structures lead to varied local renewal of reactants depending on the fluid flow conditions. Consequently, numerical models that simulate the geochemical evolution of serpentinised ultramafic rocks, must include a proper parameterisation of actual or former pathways (inferred from mineral textures) of reaction fluids. One possibility to consider realistic 3D geometries as a boundary condition for numerical simulations (e.g. Gouze & Luquot, 2011; Flukiger & Bernard, 2009; Øren & Bakke, 2003) is to characterise textures of ultramafic and serpentinite rocks by microtomography. Finally, hydrothermal vents associated with serpentinised rocks are thought to play a key role in the genesis of life in the early oceans. Whether life is possible or not, depends both on the availability of energy for metabolic processes and on the presence of cavities that are able to accommodate the organisms. Although serpentinisation processes in the temperature range of ca. 100 to 350 °C are not able to produce cavities, the subsequent seafloor alteration of serpentinites at ambient temperatures is able to dissolve certain serpentinisation products. Especially dissolution of brucite might offer ideal conditions for microbial organisms by providing them with both energy and space.

Here, we present our first results of a study on textures in serpentinised, seawater-alterated mantle rocks from the ocean floor with high-resolution X-ray microtomography.

## Method

In this study we examined a serpentinised harzburgite from the Mid-Atlantic Ridge. In the 15°N area, the Ocean Drilling Program (ODP Leg 209, Kelemen et al., 2004) took several

drillcores of serpentinised peridotites with minor amounts of gabbroic intrusions. We have chosen to perform a detailed study on a sample from Site 1270D (14°43.2702'N, 44°53.0839'W; water depth: 1816.9 m). This site is located a few kilometres east of the famous ultramafic-hosted Logatchev hydrothermal vent field, where the presence of active black smoker chimneys and elevated $H_2$ concentrations in the seawater are evidence for ongoing serpentinisation below seafloor (e.g., Sudarikov & Roumiantsev, 2000). Sample 1270D-001-01W_75-78 is from 0.75 metres below seafloor, where contact with seawater at ambient temperatures is furthermore able to dissolve the brucite that formed during the preceding serpentinisation reactions.

A tetragonal prism, 5 mm wide and 25 mm high, was cut from the sample and scanned with the SkyScan 1172 device of the experimental and theoretical petrology group at Kiel University (Germany) with a beam energy of 100 kV, a flux of 100 µA at a detector resolution of 2.54 µm per pixel using a 360 degree rotation with a step size of 0.36 degrees and 0.5 mm Al foil. The SkyScan software NRecon was used for reconstruction from the transmission images. Segmentation, and 3D image analysis on the stack of 1944 images (2044 x 2040 voxels) were done using the SkyScan software CT-Analyser. A plugin for the multi-platform free image processing package Fiji, 3D Viewer (see Schmid et al. 2010 for details), has been employed to visualise the 3D structural models of the porous structure and high density minerals. CTVox was used for visualisation and clipping of the volumetric reconstructions.

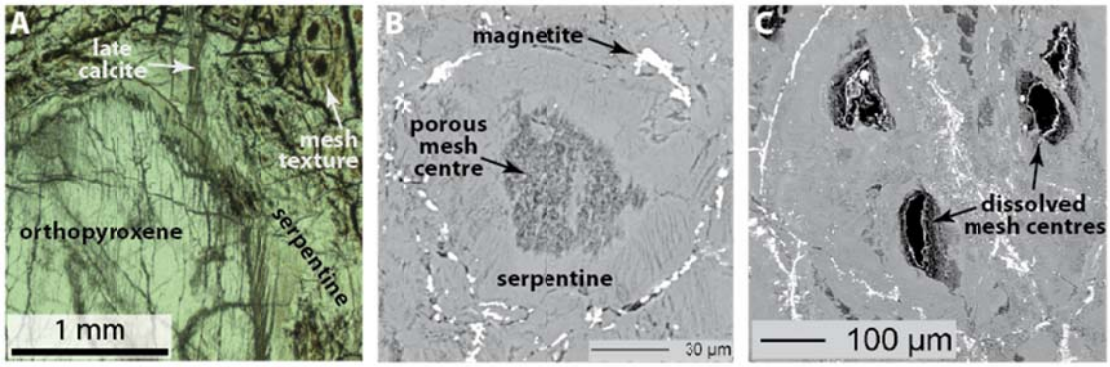


Figure 1: (A) Thin section microphotograph of the examined sample. A large orthopyroxene is rimwards replaced by serpentine. Mesh textures after primary olivine are shown in the upper right corner. The rock is crosscut by late-stage calcite veins (plane-polarized light). (B) Detailed picture (backscattered-electron image) of olivine breakdown products. Magnetite forms trails tracing former olivine grain boundaries. These meshes are filled with serpentine and brucite. Here, brucite is partly dissolved and the mesh centre becomes porous. (C) Backscattered-electron image showing completely dissolved mesh centres. Note the narrow but bright rim around holes (black). Further discussion is given in the text.

## Results

Petrographic observations show pervasive serpentinisation of the harzburgite. Primary olivine is not preserved and entirely replaced by secondary minerals in so-called mesh textures. These meshes are bordered by magnetite, which traces the former olivine grain boundaries, and filled with serpentine ($X_{Mg}$=Mg/(Mg+Fe)= 0.95-

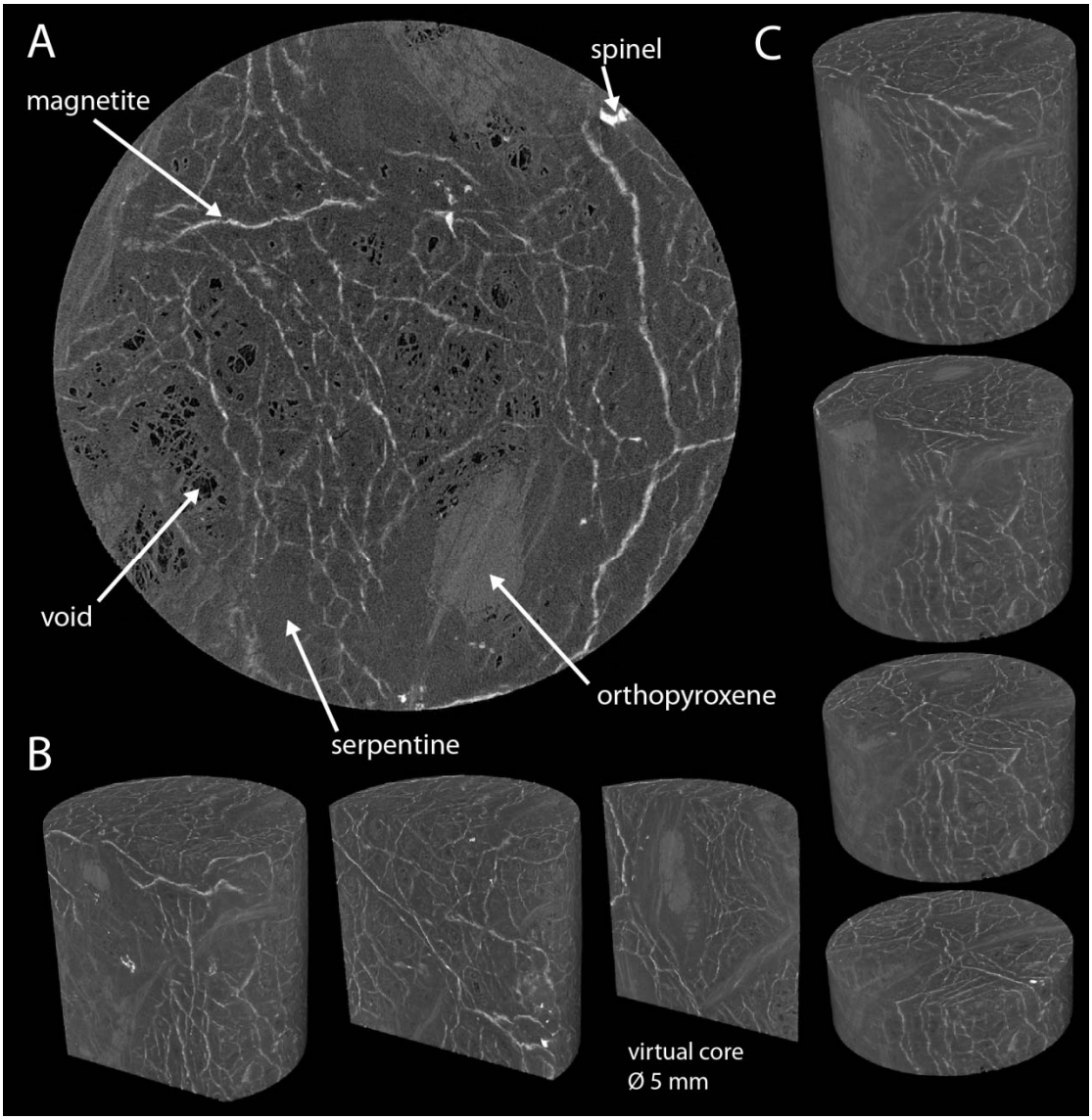


Figure 2: The virtual core of the sample exhibits a complex sequence of mineral replacement reactions. During tectonic uplift and cooling of the ultramafic mantle rocks, the original assemblage of olivine + orthopyroxene + rare spinel has been hydrated to form serpentine, brucite and magnetite. Later, low-temperature seawater alteration leads to formation of calcite veins and the development of porosity by dissolution of brucite by seawater. (A) Reconstruction image. The porous structures are created by dissolution of brucite. Relicts of primary orthopyroxene, and late-stage carbonate veins are displayed in intermediate grey levels. Trails of magnetite, grown at the borders of the mesh textures, and relict grains of primary spinel are light grey to white. (B) and (C) Volume renderings of the virtual core, cut parallel (B) and perpendicular (C) to core axis from different angles.

0.97). Typically, the centres of meshes are of brownish colour (Fig. 1A), and in X-ray element distribution maps they show lower Si and slightly elevated Fe contents. This points to the presence of brucite as breakdown product of olivine. Orthopyroxene ($X_{Mg}$= 0.91-0.92) - another primary mineral in harzburgites - is locally preserved (Fig. 1A). It breaks down to form serpentine ($X_{Mg}$= 0.90-0.92), and in the immediate vicinity of orthopyroxene, neither brucite nor magnetite is present. Additionally, Cr-rich spinel and minor amounts of tremolitic amphibole are locally observed. Besides serpentinization reaction products, late-stage lower-temperature hydrous alteration is evidenced by a network of calcite ($CaCO_3$) veins (Fig. 1A) and by development of

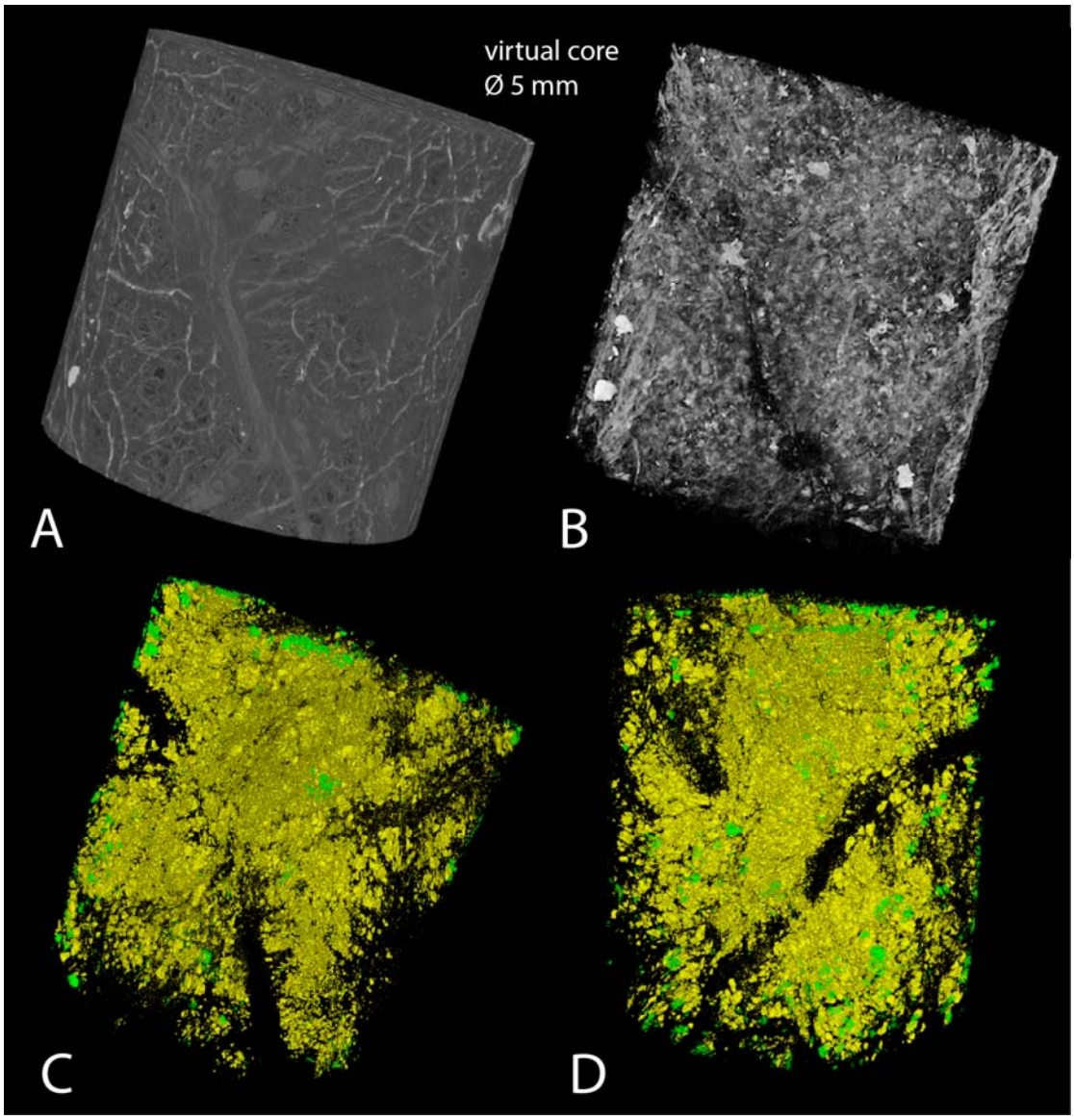


Figure 3: (A) Volume rendering of the virtual core, documenting the complex sequence of mineral replacement reactions accompanying the seafloor-alteration of serpentinised mantle rocks. (B) Maximum intensity projection visualising the location of strongly attenuating minerals. Massive white to light grey grains are spinels, a primary mineral that was preserved despite the serpentinisation and seawater alteration processes affecting the rock. The fine, spiderweb-like structures of intermediate grey levels consist of magnetite, a serpentinisation product formed at the expense of primary olivine. Calcite veins, alteration products of the late low-temperature marine weathering processes, are displayed as medium to light grey bands. (C) and (D) Visualisation of the porosity and the lack of connectivity within the porous system (green: porosity connected to the surface of the virtual core; yellow: closed porosity), (C) and (D) viewed from slightly different angles. The porous structures are caused by dissolution of brucite, a serpentinisation product, by low-temperature marine weathering processes. No porosity can be observed in areas of serpentinised primary orthopyroxene, where brucite is not expected as a breakdown product.

variable degrees of porosity in mesh centers (Figs. 1B and 1C). The latter is believed to form due to dissolution of brucite in contact with seawater. Furthermore, backscattered-electron images show bright rims around dissolved brucite mesh centres, which might consist of Fe oxyhydroxides; however, additional mineral chemical work needs to be done to prove this hypothesis.

Observations made in thin sections (ca. 25 μm thick) are one classical tool of petrographic analysis; however this techniques only allows for two-dimensional analysis of the specimen. Furthermore, grinding and polishing in the course of the thin section preparation might introduce artifact textures. To understand the fluid-rock interactions on a micro-scale and in a three-dimensional context without the drawback of preparation artifacts, X-ray microtomography presents a valuable complement. Like in petrographic thin sections, the virtual core of the sample exhibits the serpentinisation reactions, which formed during tectonic uplift and coeval cooling under hydrous conditions. In addition, the breakdown of orthopyroxene to form serpentine can now be examined in the third dimension (Fig. 2). Visualization of larger vein structures in the specimen shows a linkage between the orthopyroxene relicts. Primary olivine is replaced by a network of magnetite, which does not show a preferred orientation (Figs. 3 and 4). Microtomography also confirms the presence of voids in the centres of some mesh cells (Figs. 2 and 3), which in thin sections could have been interpreted as demolished due to polishing. Moreover, the voids display a complex internal structure, the significance of which remains to be explained. Late calcite veins crosscutting the rock can be visualized; in orthopyroxene, they follow the direction of cleavage and exsolution lamellae.

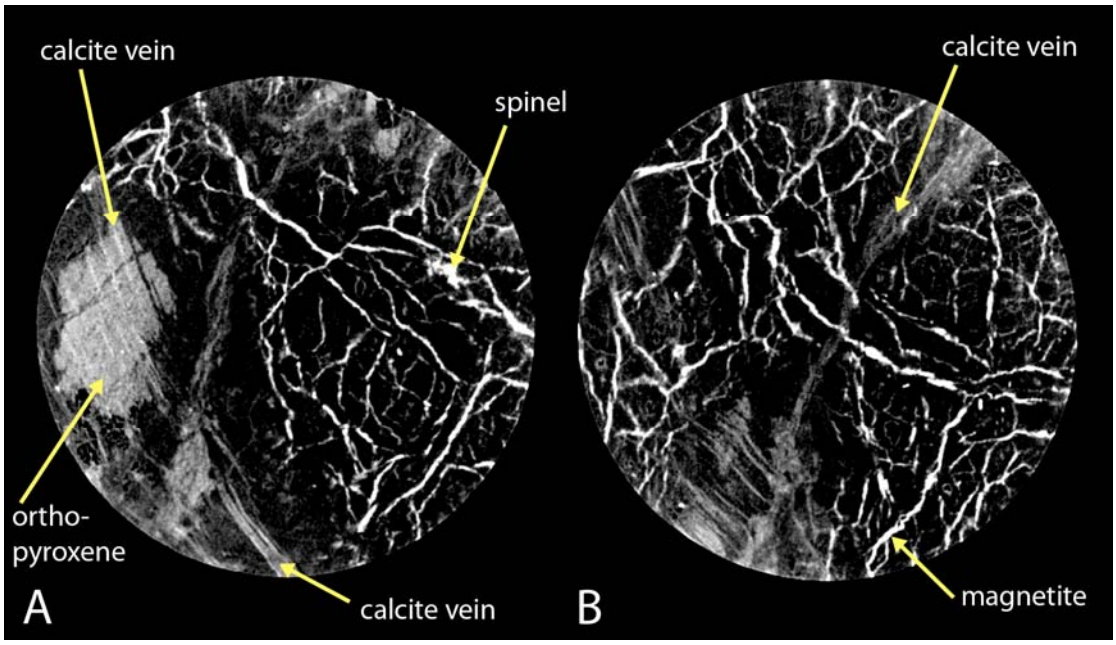


Figure 4: Reconstruction with low grey level representation of weakly attenuating minerals to enhance segmentability of the strongly attenuating phases. (A) Reconstruction images showing the network of magnetite bands (white), light grey areas of relict orthopyroxene and calcite veins.

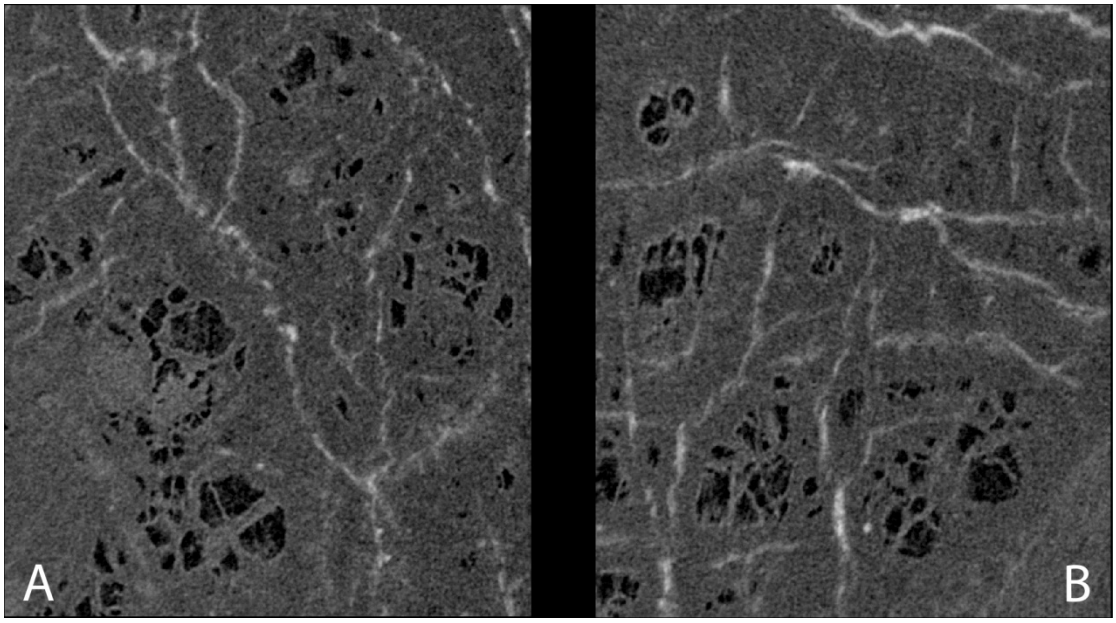

Figure 5: Close-up of the porous structures in mesh centres. (A) Image width 1.5 mm. (B) Image width 1.4 mm.

## Conclusion

Use of X-ray microtomography represents a powerful tool to visualize the three-dimensional structures of hydrothermally altered rocks from the ocean floor. While classical petrographic tools such as thin section microscopy suffer from preparation artifacts, X-ray microtomography allows analysis of undisturbed sample material and thus precludes misinterpretation of textural relations. Furthermore, insights into the true spatial arrangements of the rock fabric can further our understanding of the complex mechanisms of fluid-mineral interactions in water-rock systems.

## References:

1. Flukinger, F., and Bernhard, D., 2009. "A new numerical model for pore scale dissolution of calcite due to CO2 saturated water flow in 3D realistic geometry: Principles and first results." *Chem. Geol.* **265**, 171-180.
2. Gouze, P., and Luquot, L., 2011. "X-ray microtomography characterization of porosity, permeability and reactive surface changes during dissolution." *Journal of Contaminant Hydrology* **120–121**, 45-55.
3. Kelemen, P.B., Kikawa, E., Miller, D.J., et al., 2004. Proceedings of the Ocean Drilling Program, Initial Reports, 209 [CD-ROM]. Ocean Drilling Program, Texas A&M University, College Station TX 77845-9547, USA.
4. Øren, P.-E., and Bakke, S., 2003. "Reconstruction of Berea sandstone and pore-scale modelling of wettability effects." *J. Petrol. Sci. Eng.* **39**, 177-199.
5. Schmid, B., Schindelin, J., Cardona, A., Longair, M., and Heisenberg, M. (2010) "A high-level 3D visualization API for Java and ImageJ." BMC Bioinformatics 11:274.
6. Sudarikov, S. M. & Roumiantsev, A. B. (2000). "Structure of hydrothermal plumes at the Logatchev vent field, 14°45'N, Mid-Atlantic Ridge: evidence from geochemical and geophysical data." *Journal of Volcanology and Geothermal Research* **101**, 245-252.